Figure 4.1.3 is a plot of normative quartz content versus normative albite for the samples from this study and the Barberton area. This plot supports the suggestion that there is a progressive decrease in quartz with increasing alteration, as suggested by the R1-R2 plot. Within the albitized intrusions, especially the Discovery Shaft intrusion, there is a range of quartz-albite contents indicating that varying degrees of albitization exist. The Maranda granite plots within the altered portion of the granitoids. The samples from the Duchen Mine intrusion suggest that the body has not undergone albitization, as indicated by the high quartz content of 39% and low normative albite content of 31%.

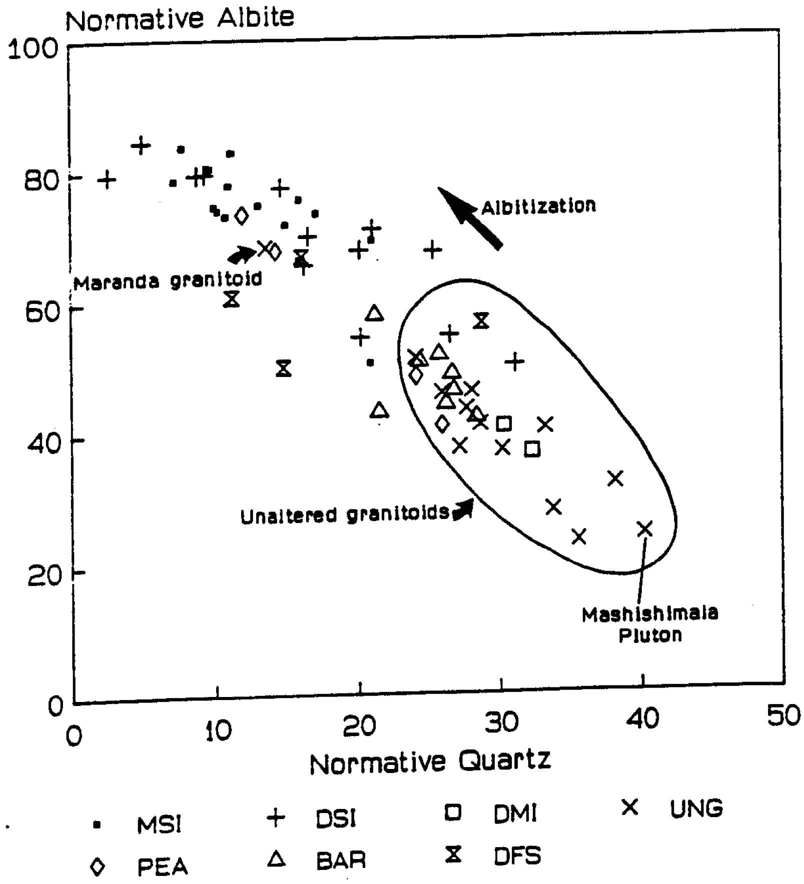

Figure 4.1.3. Normalized albite content versus quartz content.
Symbols as per Figure 4.1.1.
DFS - Discovery mine Felsites

Table 4.1.7 shows the correlation matrices for the normative mineral contents. The Malati Store and Discovery Shaft intrusions exhibit a good negative correlation between normative albite and quartz contents (r = >-0.88), as well as a negative correlation between albite and anorthite (r = >-0.61).

Malati Store Intrusion				
	QZT	ALB	ANT	P. INDEX
QZT	1.000	**-0.886**	0.516	-0.183
ALB	**-0.886**	1.000	**-0.600**	0.044
ANT	0.516	-0.594	1.000	0.134
P.INDEX	-0.183	-0.044	0.134	1.000

Discovery Shaft Intrusion					
	QZT	ORT	ALB	ANT	P.INDEX
QZT	1.000	0.471	**-0.871**	0.471	-0.229
ORT	0.471	1.000	**-0.800**	0.821	0.353
ALB	**-0.871**	**-0.797**	1.000	**-0.704**	-0.205
ANT	0.471	**0.820**	**-0.704**	1.000	0.087
P.INDEX	-0.223	0.353	-0.205	0.089	1.000

Table 4.1.7. CORRELATION MATRICES FOR CALCULATED NORMATIVE MINERALS

The "felsite intrusions" which occur within the Discovery and Cobra pits appear to be of variable composition, as indicated by the variable normative mineral compositions. They are characterised by a high anorthite content, averaging 12.12%, compared to 3.93% for the Discovery Shaft intrusion. They have lower normative quartz and albite contents than the Discovery Shaft and they are characterised by higher normative biotite contents than the Discovery Shaft intrusion. The samples of albite pegmatite also show a range of normative compositions. This variable composition is partially due to the heterogeneous and coarse grained nature of the pegmatites and the presence of biotite rich material which is closely related to the pegmatites. The pegmatites generally have a high albite content and low normative quartz content.

The albitite from BVB emerald mine contain no normative quartz and has an albite content of 79.5%. This pegmatite body is related to the emerald mineralisation at this locality.

4.1.3. K_2O and Na_2O Contents

The intrusives from this study have a wide range of K_2O and Na_2O values. The Malati Store intrusion has a low K_2O content, the average being 0.11%. The Discovery Shaft intrusion has an average K_2O content of 0.22% and a broader range of values than the Malati Store intrusion. In comparison, the unaltered granodiorite material has an average K_2O content of 3.5% although the limited data from Barton (unpubl. data) and Minnitt (1975) suggest that there is also a wide range of K_2O contents in the unaltered intrusives from this area. The albitized intrusions are very low in K_2O (< 0.2 %) and this is interpreted to suggest that there has been a large reduction in the K_2O content of the intrusions during albitization (See Section 4.1.9). The Na_2O content of the albitized intrusions is high when compared to the average content of the magmatic unaltered TTG's suite from the Murchison and Barberton belts. The Malati Store has a average Na_2O content of 8.06% and a maximum content of 9.26%. The Discovery Shaft has a lower average Na_2O content of 7.8%. In comparison, the unaltered intrusions have Na_2O contents in the range of 4.4% to 5.14%. The high Na_2O content in the altered intrusions cannot be explained by conventional igneous processes. Thus, the increase in the Na_2O content of the intrusions and decrease in the K_2O content, must be associated with the replacement of the primary igneous assemblage by albite during hydrothermal alteration.

The single analysis of the Maranda Pluton (Barton, unpubl. data) also shows a high Na_2O content (7.91%), indicative of albitization. However this intrusion also maintains a relatively high K_2O content (2.56%). This suggests that the intrusive has undergone only slight fluid interaction and alteration and hence there is no major decrease in K_2O. Alternatively, late sericitization has occurred.

The $Na_2O:K_2O$ ratios for the Malati Store intrusion exhibit a range of values from 9.51 to 280, with an average of 65. The Discovery Shaft intrusion has a lower ratio of 24.58 and ranges from 3.03 to 67.88, indicating that this intrusion has been less affected by albitization. The unaltered intrusions examined have average $Na_2O:K_2O$ ratios of 1.3. The albite pegmatites sampled have high $Na_2O:K_2O$ ratios of between 18.9 and 49.7, indicating that the fluids responsible for the pegmatites formation were enriched in Na_2O and low in K_2O.

Figure 4.1.4 is a plot of Na_2O versus K_2O content for the samples from this study. The plot shows that there is a strong negative correlation between Na_2O and K_2O contents. This is interpreted as indicating a progressive leaching of K_2O from the intrusive body with increasing albitization. The Malati Store intrusion has a very low K_2O content and high Na_2O content compared to the Discovery shaft intrusions suggesting that the Malati Store intrusion have been subjected to a more severe leaching of K_2O relative to the Discovery Shaft intrusion.

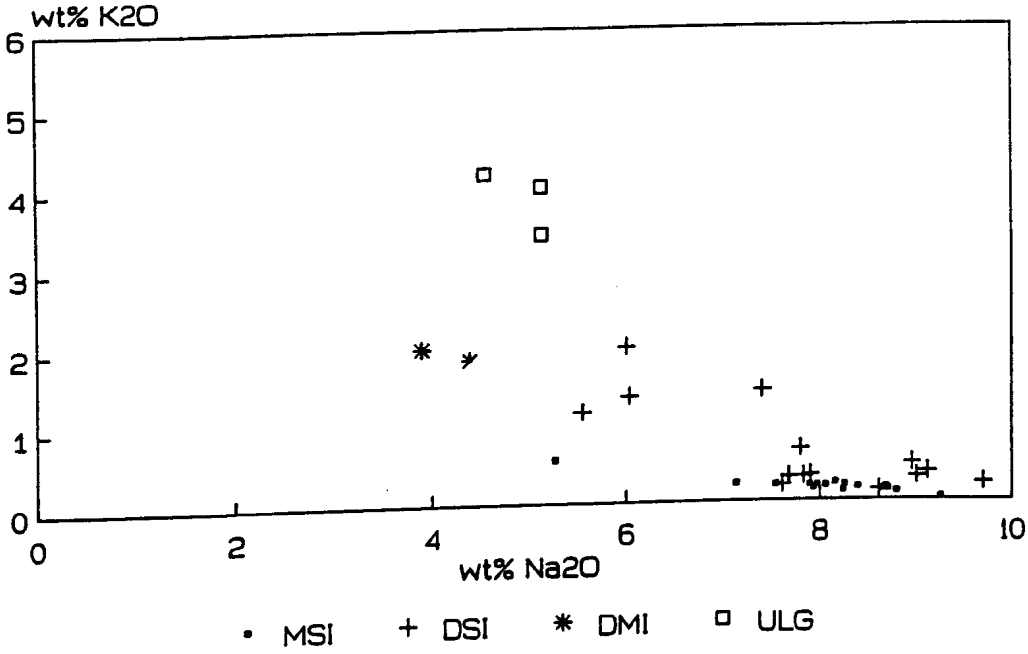

Figure 4.1.4. K_2O versus Na_2O content for the granitoids from this study
MSI - Malati Store intrusion
DSI - Discovery Shaft intrusion
DMI - Duchen mine intrusion
UNG - Unaltered granodiorites
DFS - Discovery mine felsites

Figure 4.1.5 is a plot of Na_2O versus K_2O for the samples from this study, compared to the unaltered granitoids from the Murchison and Barberton area (Glickson, 1976; Barton unpubl. data; Condie and Hunter, 1976) which shows the major fields of granitic rocks. The unaltered granitoids of the Murchison area show a wide range in compositions from granite (*senso stricto*) to tonalites. The albitized intrusions are shown to have severely depleted K_2O and enriched Na_2O contents compared to the unaltered intrusions.

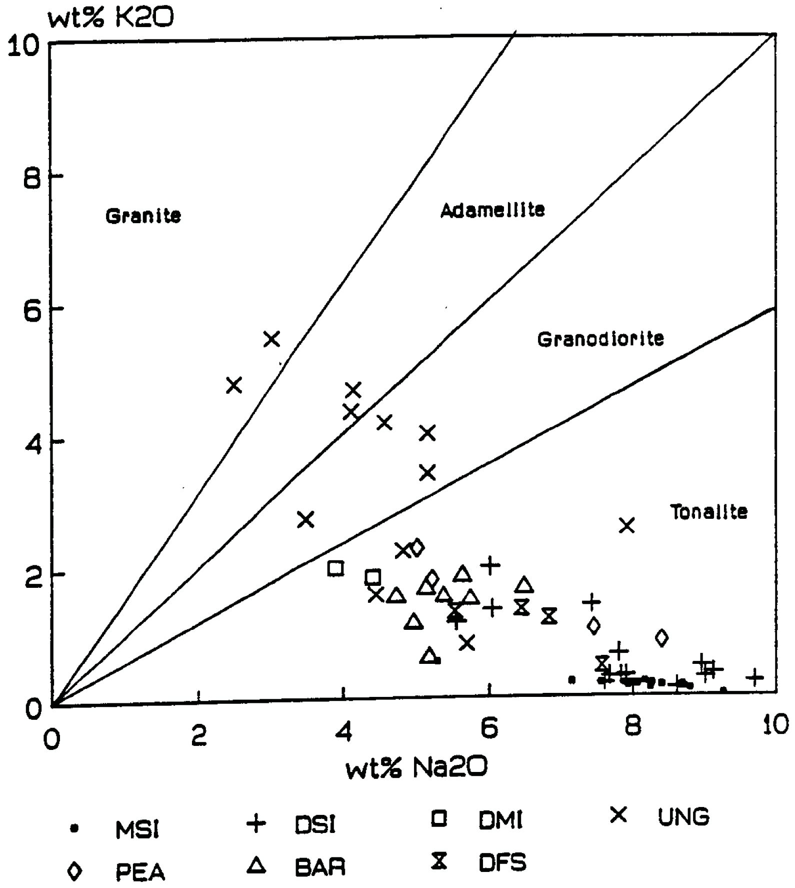

Figure 4.1.5. K_2O versus Na_2O for granitoids from the Murchison schist belt and Barberton area for comparison.
MSI - Malati Store intrusion
DSI - Discovery Shaft intrusion
DMI - Duchen mine intrusion
ULG - Unaltered Murchison granodiorites (This study; Barton, unpubl. data; Minnitt, 1975)
PEA - Albitites of Pearton (1980)
BAR - Barberton TTG's (Glickson, 1976)

4.1.4. Other Geochemical Features

The Discovery Shaft and Malati Store intrusions have slightly enriched MgO values compared to unaltered granodiorites. These intrusions average 1.0% and 1.3%, respectively, compared to 0.25% for the unaltered granodiorite. This elevated MgO content is likely to reflect small amounts of chlorite and actinolite which occur sporadically within the body especially near the rims of the intrusion, as in the case of the Discovery Shaft. The total FeO content of the altered intrusions is also elevated due to the high pyrite content of these intrusions (± 5%). The calcium content of the albitized intrusions is variable but is highly elevated compared to the Willie Pluton, although some of the other unaltered intrusions considered previously to have a higher Ca value (± 2.0%) (Barton, unpubl. data). The elevated Ca content most likely reflects epidote and carbonate phases precipitated by hydrothermal alteration.

4.1.5. Trace Element Geochemistry

The trace element contents of the intrusions from this study are presented in Tables 4.1.8, 4.1.9 and 4.1.10.

4.1.6. Transition Elements

The concentrations of transition elements (Ti, Cr, Mn, Fe, Co, Ni, Cu and Zn) have been determined for the Discovery Shaft, Malati Store and Minerva Mine intrusive granitoids. The transition elements have been plotted on a chondrite normalized diagram so that variation between samples can be observed (Fig. 4.1.6). Allegre $_{et\ al.}$ (1968) and Allegre and Michard (1974) have used this technique successfully to illustrate the effects of magmatic differentiation. Depending on ionic radii and crystal field theory (Allegre $_{et\ al.}$, 1968) as well as the existence of octahedral crystal lattice sites within early formed minerals, Co, Cr and Ni will preferentially enter the crystallographic sites in minerals such as olivine and pyroxene at the onset of magmatic crystallization. These elements are thus preferentially depleted in the residual melts and hence granites and other fractionated rocks have a characteristic "W" shape on the normalized plot of the transition elements due to these depletions. There is a consistent negative slope for the line joining the Mn and Fe points, as well as an approximately straight line relationship between the Fe-Co-Ni points (Goldschmidt, 1954). Thus the "W" shaped normative transition element distribution is characteristic of igneous rocks. The technique has been applied to the albitites to examine weather they exhibit characteristic igneous transition element distributions.

Figure 4.1.6. indicates the envelopes of distribution of the normalized transition elements for the Malati Store and Discovery Shaft intrusions, as well as the average values for the unaltered granodiorites from the Murchison area. The Malati Store and Discovery Shaft intrusions are seen to have almost identical transition element distribution patterns and abundances. The average transition element distribution for the unaltered granodiorites is also similar to that of the albitized intrusions. This suggests that the altered and unaltered granodiorites are genetically related. However the albitized portions of the intrusions are enriched in Mn, Fe, Ni, Ti and Cu, are generally depleted in Zn.

Malati Store Intrusion (MMI)															
Element	MMI.94	MM1.142	MM2.64	MM2.65	MM2.72	MM3.164	MM3.165	MM3.169	MM4.184	MM4.187	MM4.194	MUL.1	MUL.21	MUL2.65	MUL.BER	Average
Ti	0.37	0.43	0.40	0.47	0.41	0.34	0.22	0.41	0.40	0.62	0.42	0.66	0.43	0.41	0.47	0.43
V	22.28	30.01	30.52	34.12	31.50	26.59	25.24	59.47	28.48	36.86	20.60	44.69	32.89	29.87	32.40	32.30
Cr	6.01	8.27	8.53	5.93	5.54	3.78	9.55	14.62	6.29	12.26	1.41	5.63	8.12	6.26	6.34	7.23
Rb	6.62	5.86	5.69	7.81	2.59	5.73	5.35	15.82	4.16	5.89	5.57	0.480	4.26	5.12	4.12	5.96
Sr	85.95	104.87	62.64	67.84	64.48	70.61	61.48	135.80	59.84	59.03	91.10	73.10	76.89	72.54	87.45	78.25
Rb/Sr	0.077	0.056	0.091	0.115	0.040	0.081	0.087	0.116	0.069	0.100	0.061	0.066	0.055	0.071	0.047	0.08
K/Rb	302.12	153.85	333.92	281.69	733.59	261.78	56.08	347.66	132.50	220.74	287.253	333.33	281.69	429.69	242.72	302.08
Y	25.77	14.04	19.15	19.43	20.23	23.67	13.33	23.44	14.97	34.76	27.64	21.63	22.45	25.64	19.78	21.73
Zr	193.05	133.50	163.07	141.78	162.01	186.14	70.08	161.30	122.11	164.47	225.85	176.58	168.25	172.68	218.45	163.29
Nb	7.41	5.25	7.84	8.85	6.50	7.27	5.86	6.89	6.26	13.37	9.66	10.43	8.34	5.12	7.43	7.77
Co	7.27	9.28	8.87	7.53	7.63	10.96	7.47	8.02	8.64	8.88	9.03	8.76	7.71	9.58	5.92	8.37
Ni	3.82	9.47	5.64	4.93	5.59	8.62	4.08	16.38	3.66	9.17	3.44	4.55	5.11	7.14	5.51	6.48
Cu	7.81	6.46	3.63	4.61	5.67	18.11	2.37	6.25	4.89	8.74	19.67	4.86	5.69	9.25	4.23	7.48
Zn	19.40	27.40	6.55	13.09	5.56	13.38	8.22	31.14	7.36	7.53	7.75	6.86	8.10	6.32	5.99	11.64

Table 4.1.8. TRACE ELEMENT ANALYSES FOR THE MALATI STORE INTRUSION (MMI) (ppm)

Discovery Shaft Intrusion (DSI)														
Sample	KE51.6G	KE21.G	KE21.8	KE21.7	KE81.2	BH186.18 0	KE81.1	KE18.5	11.7	11.11	KE44	11.10	dis.bar	Average
Ti	0.22	0.36	0.25	0.24	0.28	0.72	0.70	0.30	0.31	0.23	0.26	0.31	0.35	0.35
V	17.01	67.37	19.29	16.54	37.88	63.35	52.21	33.31	40.93	27.08	20.12	37.98	35.45	36.04
Cr	9.21	20.80	18.23	15.70	14.21	81.86	62.54	22.74	20.16	14.87	22.12	24.51	25.98	27.90
Rb	3.14	35.46	8.50	13.07	42.97	34.49	3.14	11.52	61.72	13.76	9.89	42.97	10.23	22.38
Sr	153.15	265.96	145.50	160.59	257.26	324.67	356.83	321.50	202.41	248.54	186.54	252.86	212.76	237.58
Rb/Sr	0.021	0.133	0.059	0.081	0.167	0.106	0.009	0.036	0.305	0.055	0.053	0.068	0.048	0.09
K/Rb	414.01	394.81	233.92	168.32	311.85	133.37	366.42	250.42	320.80	210.75	303.34	81.45	312.80	290.47
Y	6.53	6.88	6.42	6.26	7.83	8.35	9.31	6.41	9.02	6.72	6.24	5.47	5.57	7.00
Zr	118.11	151.41	123.50	149.24	121.14	160.93	137.58	147.19	147.01	142.83	125.64	155.49	128.32	139.11
Nb	4.01	4.05	5.25	5.76	5.48	5.62	4.99	4.14	5.12	4.08	5.21	4.92	4.54	4.86
Co	8.47	8.74	7.31	9.20	5.83	13.39	16.14	10.07	5.51	6.99	8.95	6.38	7.45	8.92
Ni	4.65	15.05	8.65	9.86	8.65	20.47	20.36	12.38	11.42	11.25	8.12	10.91	14.72	11.81
Cu	21.44	25.74	46.33	0.82	19.89	20.14	14.57	16.56	42.66	0.20	32.45	1.13	18.31	20.16
Zn	9.59	14.11	11.15	9.28	19.14	18.39	9.04	10.67	21.67	10.51	48.21	17.04	9.45	16.57

Table 4.1.9. TRACE ELEMENT ANALYSES FOR THE DISCOVERY SHAFT INTRUSION (DSI) (ppm)

	Unaltered Granodiorites (ULG)			Discovery "Felsites" (DFS)			Cobra Pit Pegmatites (ABP)			Minerve Mine Intrusion (MMI)		Duchen Mine Intrusion (DMI)		Albitites from BVB (BVB)		Tonalitic gneiss from BVB (TON)
Element	JUD.3	MIN.2	JUD.5	DISP.2	DISP.3	D2	COB.2	COB.1	COB.3	MIN.1	MIN.4	DUC.1	DUC.2	BVB.1	JUD.2	BVB.2
Ti	0.29	0.30	0.24	0.74	0.31	0.26	0.27	0.36	0.29	0.14	0.13	0.28	0.28	0.25	0.07	0.09
V	20.42	15.21	25.42	72.70	27.38	21.90	10.45	11.54	9.58	15.56	14.19	20.21	19.54	13.87	10.06	16.84
Cr	7.02	7.71	7.45	77.06	18.31	10.62	11.76	9.49	10.56	8.19	11.40	8.43	8.21	13.91	9.48	19.27
Rb	149.90	147.82	157.11	61.23	24.06	50.27	58.55	31.45	45.89	3.01	6.44	85.23	80.12	2.51	9.45	58.72
Sr	420.37	351.97	342.67	821.66	794.06	315.73	172.76	158.98	168.95	198.64	158.03	542.32	495.39	166.69	77.64	683.58
Rb/Sr	0.357	0.420	0.458	0.075	0.030	0.159	0.339	0.198	0.272	0.015	0.041	0.157	0.162	0.015	0.122	0.08
K/Rb	267.51	230.68	266.05	195.98	191.27	260.60	295.06	426.07	344.12	265.78	170.81	215.89	248.38	187.25	603.2	118.8
Y	6.99	5.45	7.25	10.20	7.34	7.02	8.49	6.98	7.23	10.27	6.93	4.54	3.89	14.91	14.43	6.44
Zr	144.98	147.56	135.45	168.20	157.14	127.81	101.52	134.71	155.21	102.17	70.47	73.32	71.10	116.98	46.35	89.64
Nb	3.44	10.84	5.21	5.64	0.44	4.26	7.03	5.87	6.38	4.33	8.83	2.45	3.21	5.41	10.28	7.92
Ce	10.30	6.21	9.86	9.81	10.44	7.48	5.57	9.99	5.12	6.63	5.87	10.54	15.84	8.41	7.24	9.20
Ni	7.23	4.44	8.20	22.38	8.91	19.74	10.32	2.51	5.69	2.90	6.30	4.97	8.29	2.97	0.44	13.46
Cu	0.87	0.67	0.79	7.96	13.10	41.21	5.52	5.48	8.59	15.47	19.65	1.96	0.86	0.48	0.26	8.76
Zn	26.13	27.49	23.21	35.74	32.74	19.78	10.64	7.56	9.95	7.35	10.87	25.12	30.15	6.47	9.43	18.35

Table 4.1.10. TRACE ELEMENT ANALYSES FOR VARIOUS GRANITOIDS FROM THE MURCHISON AREA (ppm)

The enrichment of Fe and Cu is attributed to the development of pyrite and chalcopyrite mineralization within the altered portions. All the intrusives have characteristic transition element plots for typical granitic material (Allegre and Michard, 1974). Figure 4.1.7. contains the envelopes of distribution of the transition elements for the TTG suite of the Barberton area, as well as average values for the Discovery Shaft and Malati Store intrusions. There is a close similarity between the albitites of the Murchison belt and the Barberton TTG's. The transition element plot exhibits features that are characteristic of fractionated igneous rocks, a feature which argues against a lateral metamorphic secretion genesis for the albite rich rocks.

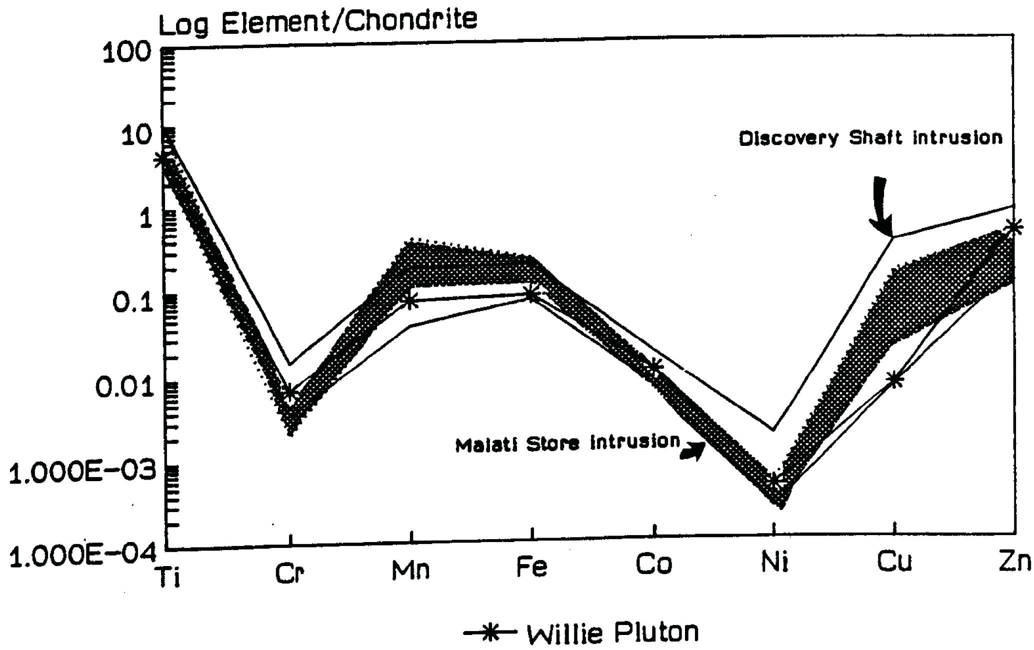

Figure 4.1.6. Chondrite normalized transition element plots showing the envelope of distribution for the Discovery Shaft and Malati Store intrusions as well as the average composition of the unaltered Willie pluton

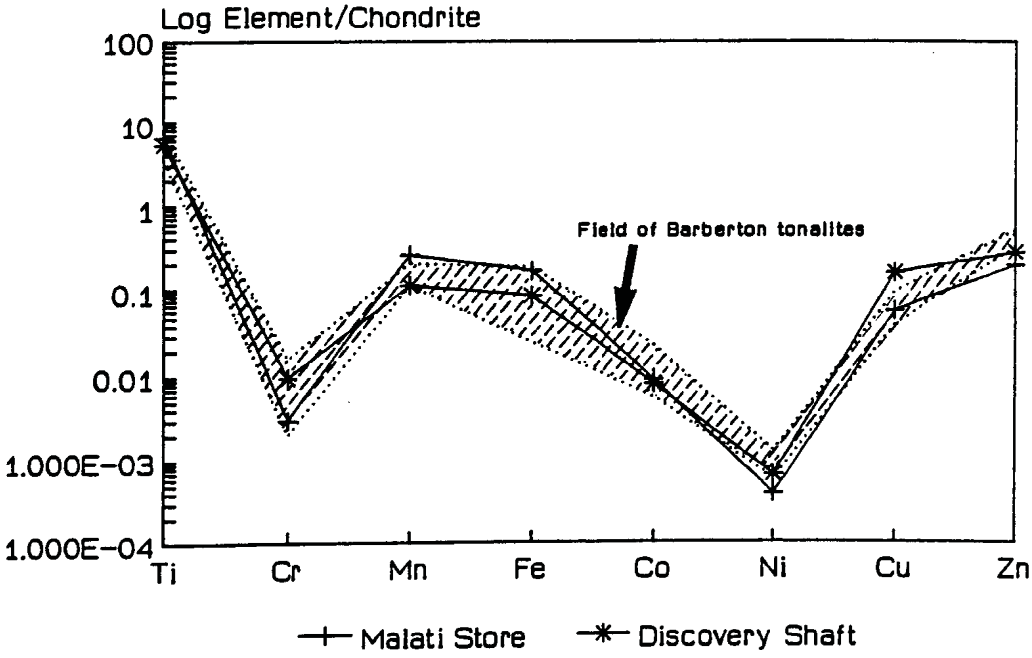

Figure 4.1.7. Average chondrite normalized transition element plots for Malati Store (MSI) and Discovery Shaft intrusions (DSI). The field of distribution of Barberton tonalites is included for comparison.

Figure 4.1.8. is a plot of the normalized transition element content for the albitite samples of Pearton (1980) (Table 4.1.1), the unaltered Willie intrusion and samples of albite pegmatite. The albite pegmatites and the albitites of Pearton (1980) have similar, characteristic, igneous transition element distributions. There is a distinctive Cr and Ni depletion in both suites, as well as an enrichment in Cu, compared to the unaltered granodiorite - as would be expected in highly fractionated igneous derived material. It is therefore suggested that the samples of albitite analyses by Pearton (1980) have the transition element distribution characteristics of the albite pegmatites which are common along the southern flank of the schist belt.

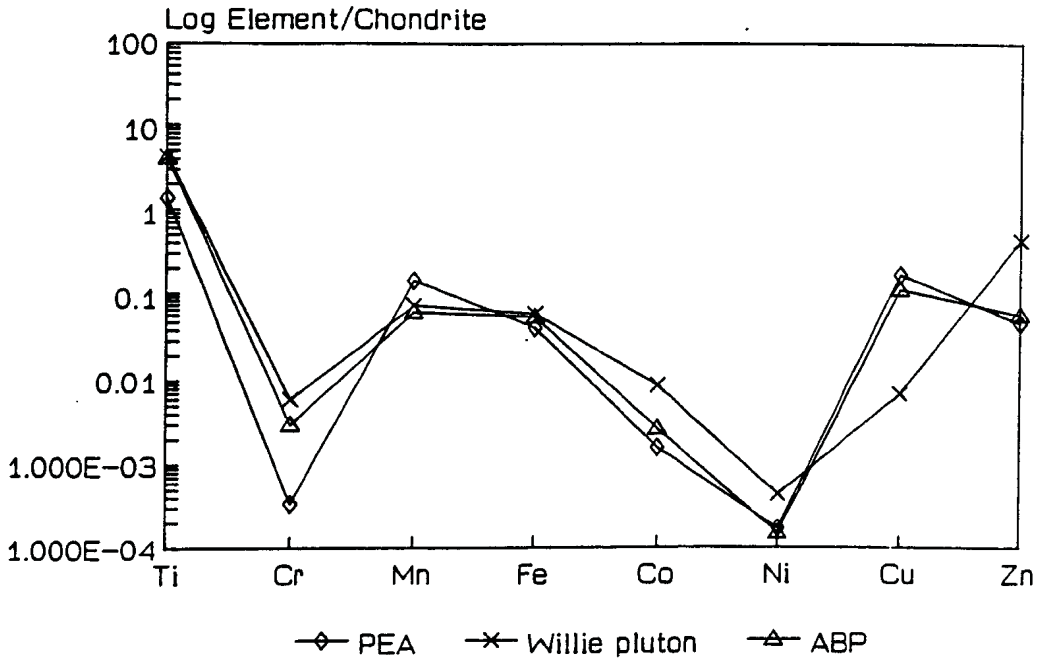

Figure 4.1.8. Chondrite normalized transition element plots for the albitites of Pearton (1980) (PEA) and the albite pegmatites from GEM (ABP). The Willie pluton is included for comparison.

4.1.7. Rb-Sr Content

The Rb and Sr contents of the Malati Store and Discovery Shaft intrusions exhibit a wide range of values. Figure 4.1.9 is a plot of Rb versus Sr for the altered intrusions, as well as the Rb and Sr contents from unaltered intrusives in the Murchison area (this study and Minnitt, 1975). The Malati store intrusion has low Rb contents (4.80 ppm to 15.82 ppm, average 5.76 ppm) and Sr contents (61.48 ppm to 135 ppm average 78.25 ppm). The average Rb/Sr ratio is 0.70. The Discovery Shaft intrusion has higher Rb (3.14 - 61.75 ppm, average 22.37 ppm) and Sr values (145.50 - 356.83 ppm, average 237.58), as well as greater ranges. The average Rb:Sr ratio of the Discovery Shaft intrusion is however, similar to the Malati Store intrusion. The Rb-Sr content of the albitized portions of the Minerva mine intrusion plot within the range of the highly albitized samples from the Discovery Shaft intrusion. The highly albitized Malati Store intrusion has a small range of Sr and Rb values, with lower levels than those of the Discovery Shaft intrusion, a feature which is expected with the higher intensity of albitization.

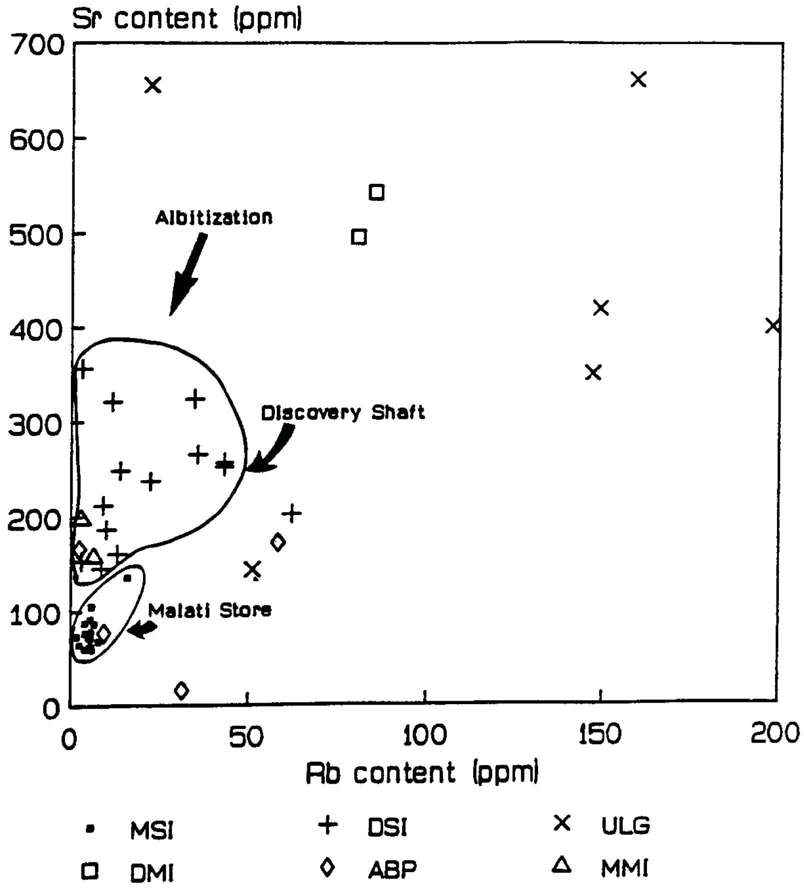

Figure 4.9. Sr versus Rb content for the granitoids of the study
MSI - Malati Store intrusion
DSI - Discovery Shaft intrusion
ULG - Unaltered granodiorites
DMI - Duchen mine intrusion
ABP - Albite pegmatites from Cobra Pit
MMI - Minerva mine intrusion

The albite pegmatites have variable Rb and Sr contents and generally plot within the zone defined by altered intrusives. The apparent decrease in the Rb and Sr content of the intrusions with increased alteration, suggests that the hydrothermal system was open and that Rb and Sr was leached from the system. This idea is supported by Figure 4.1.10, a plot of normative albite content versus Sr content, which indicates a definite negative relationship between the normative albite content (degree of alteration) and the Sr content. The trend is markedly contrary to normal igneous differentiation trends where Sr and plagioclase are positively correlated. The Malati intrusion appears to indicate higher degree of Sr and Rb leaching compared to the Discovery intrusion, similar to the observed trend of K_2O leaching.

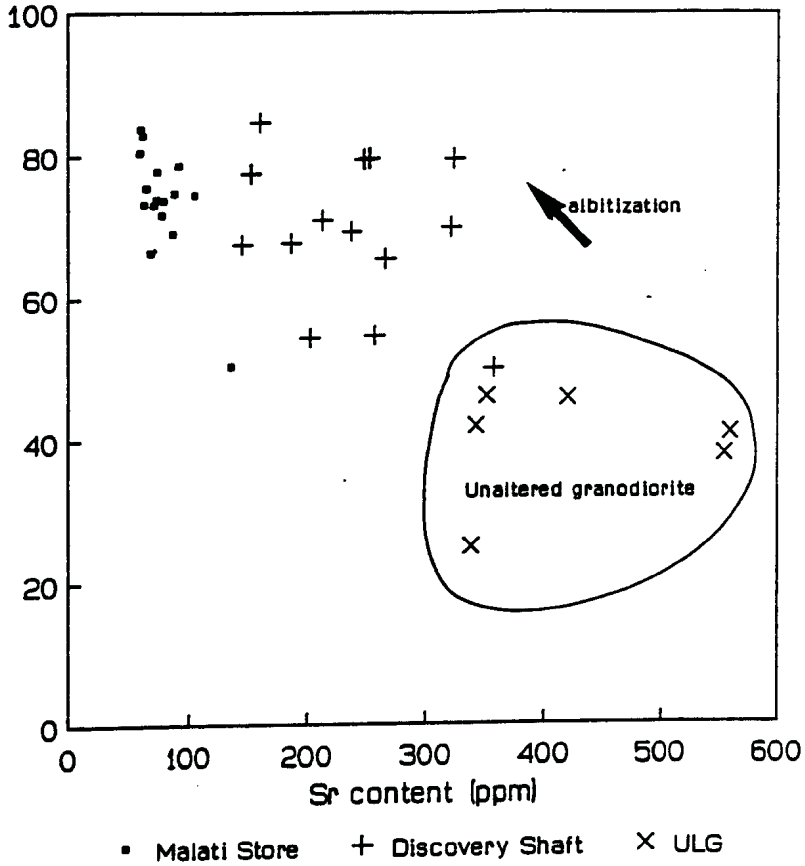

Figure 4.10. Normative albite content versus the Sr content for the Murchison granitoids studied.
ULG - Unaltered granodiorites

4.1.8. Gold, Uranium and Thorium Contents

Table 4.1.11. shows the NAA determinations for U, Th and Au contents of the albitized intrusives, the unaltered granodiorites, an albite pegmatite and a Discovery Shaft felsite. The Malati Store intrusion is highly enriched in gold, with a range of 1400-6960 ppb and an average of 3530 ppb (3.5 g/t) for the four samples analysed. This compares well with the average gold content of the intrusion as determined by Phelps Dodge (per. com) of 3.1 g/t. The Discovery Shaft intrusion has a range of 40-3140 ppb and an average of 758.8 ppb (0.75 g/t) for five samples. Underground sampling of the Discovery intrusion by GEM mine personnel were analysed for gold by standard atomic absorption techniques (Golden Dumps Research) and indicated erratic gold mineralization with values ranging from 0.25 g/t to 15.23 g/t. The Minerva mine intrusion, the albite pegmatites and the Discovery felsites have similar low gold values of 10-18 ppb. The Willie and the unaltered granodiorite at Minerva mine have gold contents of 13 ppb and 10 ppb respectively. Thus all the granitic rocks examined are enriched in Au, relative to typical Archaean granitoids. Saager and Meyer (1983) derived a figure of 2.5 ppb for typical granitoids from an evaluation of data from the Barberton area. This indicates that the intrusive granodiorite suite examined are a potential source of gold mineralization.

No enrichment of uranium and thorium occurs within the samples examined. The uranium contents are generally less than 4 ppm and the thorium content less than 7 ppm. Meyer *et al.* (1987) regards values in excess of 6 ppm uranium to represent enrichment.

Malati Store Intrusion (MSI)			
Sample	**Au (ppb)**	**U (ppm)**	**Th (ppm)**
MM1.94	6960	4.00	5.10
MM1.142	1400	3.23	6.40
MUL.1	2290	5.32	4.60
MUL.2	3550	2.73	5.40
Discovery Shaft Intrusion (DSI)			
Sample	**Au (ppb)**	**U (ppm)**	**Th (ppm)**
11.11	3140	3.88	1.40
11.7	425	5.12	3.60
KE.51.7	62	5.46	5.40
KE.81.2	127	4.24	5.80
BH186.180	45	6.30	4.90
Minerva Mine Intrusion (MMI)			
Sample	**Au (ppb)**	**U (ppm)**	**Th (ppm)**
MIN.1	13	3.40	3.50
MIN.4	10	1.45	2.20
Unaltered Granodiorites (ULG)			
Sample	**Au**	**U**	**Th**
JUD.3	10	2.20	4.30
MIN.2	8	4.50	2.40
Albite Pegmatites (ULG)			
Sample	**Au**	**U**	**Th**
COB.2	18	4.80	6.50
Discovery Felsites (DFS)			
Sample	**Au**	**U**	**Th**
D.2	15	3.79	4.30

Table 4.1.11. GOLD, URANIUM AND THORIUM CONTENTS OF THE MURCHISON GRANITOIDS

4.1.9. Alteration Studies

The percentage change in volume and concentration of mobile elements within the intrusions during albitization have been calculated using the technique of Grant (1986), which is an alternative graphical solution for the composition-volume relationships of Gresens (1967). Following the indications from the petrographic and geochemical data, the Willie Pluton has been used as the unaltered protolith against which the albitized cupolas have been normalized. Data from this study and Barton (unpubl. data) were used to produce the average composition of this intrusion.

The basic hypothesis of Gresens' (1976) is that some components are likely to have been immobile in the alteration process and, if these can be identified, they can be used to establish any volume changes which might have taken place. Gains and / or losses of components can then be calculated, assuming that the volume change is a factor common to the behaviour of all the components. A pre-requisite is that the alteration is pervasive and not confined to veins or alteration patches. Petrographic work and major element geochemistry indicate the albitization is pervasive and thus the technique may be applied.

The immobile elements are obtained graphically by plotting the major and trace element concentrations of the Willie pluton against those of any given intensely albitized sample. The immobile elements generate a straight line through the origin with a slope which is the fundamental ratio of equivalent masses before and after alteration. This line is called an isochron, and is defined as a line connecting points of equal geochemical concentration (Gary *et al.*, 1974). The relative gains and losses of (mobile) components are given by the displacement of data points from the reference isochron. The density of the granitoid material was determined by standard techniques.

The average density of the Malati Store samples is 2.77 g/cm^3 (n = 6) and of the Discovery Shaft intrusion, 2.71 g/cm^3 (n = 5). The unaltered Willie intrusion has an average density of 2.59 g/cm^3 (n = 3). There is therefore, an increase in density with increasing degrees of albitization, which equates with an increase in mass at constant volume.

4.1.9.1 Discovery Shaft Intrusion

The plot of unaltered versus altered granitoids chemical composition demonstrates that Al_2O_3, Y, Ni and Zr define a multicomponent isochron which corresponds to the constant alumina isochron. The slope of this line yields $M^o/M^a = 0.96$, which indicates a mass increase of some 4% due to albitization.

On the assumption of constant alumina content and that of constant volume (using the density data), the gains and losses of mobile components can be calculated as follows.

If constant alumina is assumed,
Concentration Change = $(M^o/M^a)*(Ci^a/Ci^o)-1$
If constant volume is assumed,
Concentration Change = $(p^a/p^o)*((Ci^a/Ci^o)-1$

Ci^a = Concentration of element in altered material
Ci^o = Concentration of element in original material
M^o = Reference mass of original material
M^a = Reference mass of altered material
p^o = Density of original material
p^a = Density of altered material

Table 4.1.12. shows the changes in concentration of mobile element for the albitized Discovery Shaft intrusion. There is only a slight difference in the element concentration changes calculated in terms of either constant alumina or constant volume. The changes in concentration during albitization for the Discovery shaft range from -90% for K_2O to +325% for Cr. Other major changes include the $Fe_{(total)}$ content which increases by 117% the Cu content which increase by 3025% and the Ti content which increases by 109%. The Rb and Sr contents are reduced by 89% and 50% respectively (Table 4.1.12). The silica and potassium contents are reduced by 5% and 90% respectively while the sodium content is increased by 57%.

4.1.12.2 Malati Store Intrusion

Major and trace elements concentrations from highly albitized portions of the Malati Store intrusion plotted against the Willie intrusion demonstrate that there is a choice of isochrons close to the constant volume and constant mass line. The gains and losses of mobile elements is thus calculated, assuming constant volume and using the formula and average densities described above (Table 4.12).

The concentration changes for the Malati Store intrusion are similar to those of the Discovery Shaft intrusion. The sodium content increases by 16% while the silica and potassium contents decrease by 16% and 96% respectively, reflecting the higher degree of albitization and desilicification within this intrusion. The Rb and Sr contents are also reduced, by amounts similar to that of the Discovery Shaft intrusion. There is a larger increase in the Fe_{Total} content (275% versus 117%) which is associated with the higher pyrite content of the Malati Store intrusion.

The similar increases (150% and 108%) in the Ti content in the two intrusions suggests that rutile/ilmenite introduction occurred early in the hydrothermal alteration, a feature which confirms the petrographic study.

Differences between the intrusions include the Y immobility in the Discovery Shaft intrusion and the 150% Y increase in the Malati Store intrusion. There is 325%, increase in Cr in the Discovery Shaft intrusion, but a 5% decrease in the Malati Store intrusion. The higher Cr in the Discovery Shaft intrusion is attributed to the presence of actinolite-chlorite and a possible interaction with the mafic and ultramafic schists.

The large increase in Cu content of the Discovery Shaft intrusion (3025%) is attributed to the chalcopyrite content of the intrusion, which is confirmed by petrographic work. The gold content of the Discovery Shaft and Malati Store intrusions has been increased by 110% and 350% respectively compared to the unaltered Willie pluton.

In summary, the process of albitization is characterised by an increase in the Ti, Fe, Mg, Na_2O, CaO, V, Cr, Nb, Ni, Cu, Au and As content and a decrease in the K_2O, P_2O_5, Rb, Sr and Zn contents of the intrusions studied. The larger elemental changes in the Malati Store intrusion confirm the greater degree of albitization as indicated by the petrographic and major element study. Thus the large element changes indicated are not the result of significant volume or mass changes.

4.1.10 Major and Trace Element Comparisons

Figure 4.11 is a spidergram plot of the major and trace contents of the Malati and Discovery intrusions normalised to an average unaltered granodiorite for the Murchison area (Data from this study; Minnitt, 1975; Barton unpubl. data). The spidergram plots for the two intrusions show that there are distinct similarities in the chemistry of both intrusions relative to unaltered granodiorite, in particular, depletions in K_2O and Rb. The Malati Store intrusion shows a greater depletion in these elements, indicating a more intense degree of alteration. Both intrusions show an increase in the Na, Cu, Ti, Ca, and Mg content relative to the unaltered granodiorite.

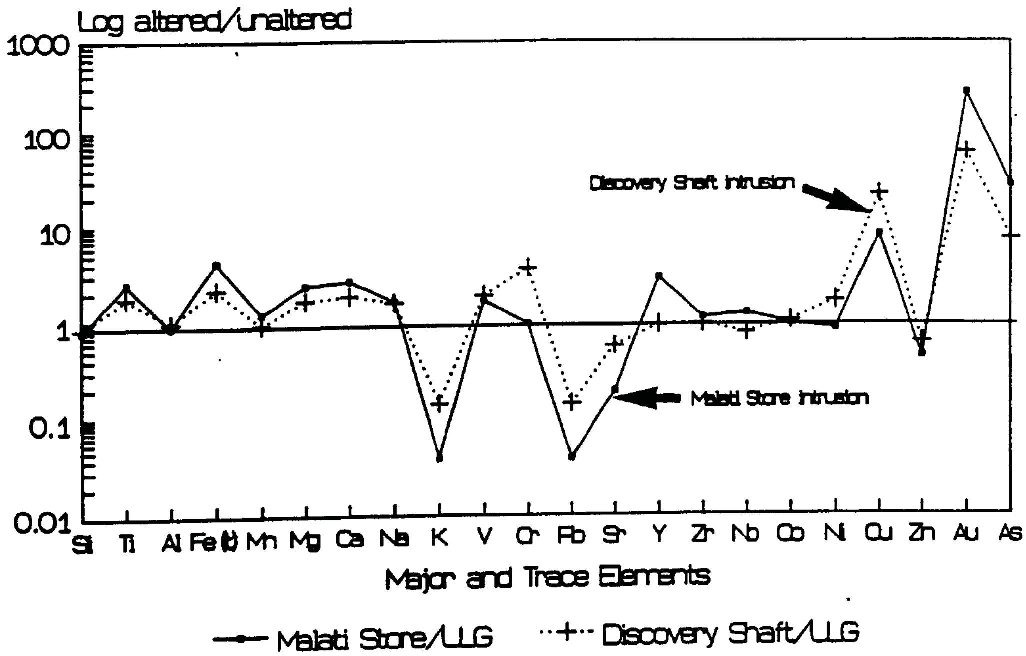

Figure 4.1.11. Log of the major and trace element contents of the average Malati Store (MSI) and Discovery Shaft (DSI) intrusions normalized to an average unaltered Murchison granodiorite (ULG)

4.1.14. Volatile Contents

Table 4.1.13. shows the CO_2, H_2O and sulphur contents of the Discovery Shaft and Malati Store intrusions, as well as the Willie pluton. The Malati Store intrusion has a high CO_2 content (average = 4.19%), which confirms the high carbonate content of this intrusion. The Discovery Shaft and the Minerva Mine intrusions have lower CO_2 contents of 1.33% and 1.23%, respectively. The H_2O content is similar in all three intrusions. The sulphur content of the Malati Store intrusion is high (average = 1.59%) while the Discovery Shaft and Minerva mine intrusions have lower sulphur contents, indicative of their lower sulphide contents. The unaltered Willie intrusion has low volatile contents, in comparison to the albitized intrusions.

Malati Store Intrusion (MSI)			
Sample	CO2 %	H2O%	S (SQ) %
MUL.1	2.00	0.65	1.61
MM4.197	7.20	0.70	1.99
MM2.65	4.05	0.71	1.73
MM1.94	3.51	0.55	1.13
MM3.82.8	3.27	0.71	1.56
MM2.64	5.08	0.65	1.51
Average	4.19	0.66	1.59

Discovery Shaft Intrusion (DSI)			
Sample	CO_2 %	H_2O %	S (SQ) %
KE.81.2	1.51	0.84	0.28
BH.186	1.89	2.42	1.01
KE.12G	0.95	1.43	0.23
KE.51.6	1.12	1.02	0.49
KE.21.18	0.55	0.93	0.32
KE.11.11	2.28	0.73	0.50
KE.11.7	1.81	0.69	0.21
KE.51.7	1.25	0.96	0.49
Average	1.42	1.13	0.44

Minerva Mine Intrusion			
Sample	CO_2 %	H_2O %	S (SQ) %
MIN.1	1.09	0.70	0.22
MIN.4	1.25	0.85	0.56
Average	1.17	0.78	0.39

Willie Intrusion (unaltered)			
Sample No.	CO_2 %	H_2O %	S (SQ) %
WIL.1	0.05	0.37	0.06
WIL.2	0.12	0.54	0.05
WIL.3	0.41	0.35	0.23
Average	0.19	0.42	0.11

Table 4.1.13. CO_2, H_2O AND SULPHUR CONTENTS OF THE MALATI STORE, DISCOVERY SHAFT AND MINERVA MINE INTRUSIONS AS WELL AS THE UNALTERED WILLIE PLUTON

4.1.12. Relationship Between Sodic and Potassic Alteration

As described earlier, a spatial relationship between potassic and sodic alteration is commonly observed in gold mineralized areas. A process proposed by Smirnov (1976), suggests that the potassium liberated during albitization is removed to upper levels in the hydrothermal system, resulting in potassic alteration. Section 4.1.9. has demonstrated that large quantities of potassium are liberated during albitization of the cupola zones of the Murchison schist belt granodiorites. It is conceivable that the liberated potassium is responsible for some of the potassic alteration observed in close proximity to the albitized intrusions.

4.1.13. Conclusion

The albite-rich rocks of the Murchison schist belt show distinct geochemical trends which project to a parental affinity with the intrusive granodiorite suite. There is a continuous geochemical progression from relatively unaltered granodiorite material to highly albitized material (albitite) within a single altered intrusion, indicating that the albite rich portions of the intrusions are the result of endogenous sodium metasomatism. The geochemistry of the albitized intrusions has a distinctly magmatic signature which precludes a metamorphic lateral secretion process for their formation. The "albitites" of Pearton (1980) show major and trace element geochemistry which is similar to that of the albite rocks examined in this study and they show transition element distributions indicative of fractionated magmatic rocks.

The fluids responsible for albitization have also been responsible for sub-economic concentrations of gold and associated metallic mineralization within the intrusions acting over large areas of the schist belt, in different geological settings. Albitization affects the cupula zones of the granodiorite intrusions which have intruded the Murchison schist belt, especially along structural discontinuities, including the Antimony Line. The ...lization of the granodiorites is therefore interpreted to be the

4.2. Rare Earth Element Geochemistry

4.2.1. Introduction

The rare earth elements (REE) lanthanum to lutetium (atomic numbers 57-71) are members of Group IIIA in the periodic table and all have similar chemical and physical properties (Haskin *et al.*, 1966; 1968; Cotton and Wilkinson, 1966). Systematic differences occur as a result of a progressive decrease in their ionic radii (of the trivalent cations) from La to Lu. Only cerium ($Ce^{+3,} Ce^{+4}$) and europium (Eu^{+3}, Eu^{+2}) exhibit oxidation states other than +3 in nature. This results in Eu^{+2} preferentially substituting for Sr^{+2}, particularly in feldspars. The ionic radii of the REE decrease with atomic number from 1.14Å for La to 0.85Å for Lu. This is known as the "lanthanide contraction" and, as a result, heavy rare elements (HREE), (Gd to Lu) have larger ratios of charge to atomic radius and generally form stronger bonds than do light rare earth elements (LREE) (La to Sm). These elements behave coherently during most geological processes because of their similar chemical properties. The fractionation which is observed occur as a result of either contraction effects on bond strength or because of anomalous valances of Eu and Ce. Of the major rock-forming elements, only Ca^{+2} and Na^{+} have similar ionic radii for eight-fold coordination states. Substitution for Na^{+} does not appear to occur normally as a result of charge imbalance (Taylor *et al.*, 1982). The LREE tend to be excluded from common rock-forming minerals during igneous processes due to their large radii and high charges and they are generally included in the group of incompatibles or large ion lithophile elements (LIL) (Herrmann, 1970). The HREE are, by virtue of their smaller ionic radii, are somewhat compatible with minerals such as zircon (Nagasawa and Schnetzler, 1970) and this may exert a fundamental influence on their distribution. Eight REE were determined by instrumental (epithermal) neutron activation techniques. Precision and accuracy for all the elements were ± 5% or 0.1 ppm, whichever was greater. Lutetium concentrations were generally at or below the detection limit for this element. The REE data is presented in the form of Masuda-Coryell diagrams, where the concentrations are normalized to abundances in chondritic meteorites (Masuda, 1962; Coryell *et al.*, 1963). The advantages of this technique include the elimination of the abundance variation between odd and even numbered REE atomic numbers and the determination of the extent of any fractionation amongst various REE, since there is no fractionation between light REE and heavy rare earth elements in chondrites (Haskins *et al.*, 1968). This procedure allows for clear presentation of inter-element fractionation and of the anomalous behaviour of any particular element in the series. For the purpose of this study, the average REE abundance for chondritic meteorites are those from Haskins *et al.* (1968), namely:-

La	0.330 ppm
Ce	0.88 ppm
Nd	0.60 ppm
Sm	0.181 ppm
Eu	0.069 ppm
Tb	0.047 ppm
Yb	0.200 ppm
Lu	0.054 ppm

4.2.2. Samples

Samples from the Malati Store, Discovery Shaft and Minerva Mine intrusions were selected to provide an indication of REE distribution with varying degrees of albitization. Analyses of the Willie pluton and the unaltered granodiorite at Minerva mine area were also undertaken to determine the relationship between the unaltered and albitized intrusions. Albite pegmatites from the Cobra pit were analysed to examine the relationship between the granodiorite intrusions and the pegmatites associated with emerald mineralization. As a result of a lack of REE data for the granitoids in the Murchison area, the intrusive granitoids of the Barberton area were also used as an alternative for a comparative study. These included the Kaap Valley Tonalite and the Theespriut pluton (Condie and Hunter, 1976 and Glickson, 1976).

4.2.3. Results

The results of the chondrite-normalised REE distribution patterns for all the samples analysed are presented in Table 4.2.1. along with the data from Pearton (1980) and characterised by a low total REE content, and are consistently LREE enriched with a linear slope. No significant europium anomaly was detected. The Malati Store intrusion has a shallow uniform slope (La/Yb_n = 4.39) and a low total rare earth content. A slightly positive europium anomaly (Eu/Eu^* = 1.09) exists and the five samples analysed exhibit limited variance (Figure 4.2.1). The Discovery Shaft deposit shows a moderately steep linear slope (La/Yb_n = 30.6) and low total rare earth content, with samples exhibiting a narrow variance and a slightly negative europium anomaly Eu/Eu^* = 0.71.

Sample	La	Ce	Nd	Sm	Eu	Tb	Yb	(La/Yb)c	Eu/Eu*
Malati Store Intrusion (MSI)									
MM4.197	7.45	23.20	16.42	2.48	1.20	0.64	1.85	2.4	1.25
MM2.65	12.80	26.94	9.56	3.06	1.10	0.60	1.43	5.4	1.07
MM1.94	15.77	25.70	15.32	3.54	1.04	0.67	1.67	5.7	1.16
MM1.142	7.01	24.33	14.60	2.79	0.93	0.36	0.99	4.3	1.19
MM1.183	11.45	25.17	14.10	2.87	1.11	0.56	1.69	4.1	1.05
Average	**10.90**	**25.07**	**14.12**	**2.95**	**1.07**	**0.57**	**1.53**	**4.4**	**1.09**
Discovery Shaft Intrusion (DSI)									
KE21.21	14.07	43.01	12.01	2.03	0.45	0.20	0.45	18.8	0.84
11.11	38.43	48.27	12.50	3.42	0.40	0.18	0.44	52.9	0.55
11.7	23.36	47.27	13.18	3.02	0.62	0.32	0.58	24.5	0.76
KE51.2	21.45	42.80	12.40	2.53	0.47	0.21	0.39	33.7	0.74
KE51.7	19.33	39.67	11.70	2.35	0.50	0.22	0.41	28.7	0.83
BH.186	24.24	46.20	13.20	3.27	0.54	0.29	058	25.2	0.64
Average	**23.48**	**44.54**	**12.50**	**2.77**	**0.50**	**0.24**	**0.48**	**30.6**	**0.71**
Minerva Mine Intrusion (MMI)									
MIN.1	13.10	31.79	12.78	2.87	1.04	0.20	0.60	13.3	1.49
MIN.3	12.55	30.21	12.30	2.79	0.68	0.29	0.42	18.2	0.93
MIN.4	12.82	31.30	12.52	2.82	0.66	0.25	0.52	14.9	0.90
Average	**12.82**	**31.10**	**12.53**	**2.83**	**0.79**	**0.25**	**0.51**	**15.5**	**1.04**
Unaltered Granodiorite (ULG)									
MIN.2	15.14	28.44	8.54	1.88	0.66	0.23	0.56	8.0	1.02
JUD.3	13.85	30.10	8.50	1.83	0.40	0.16	0.38	11.9	0.86
Albite Pegmatites (ABP)									
COB.1	22.14	38.45	12.50	2.56	0.52	0.30	0.98	13.7	0.74
COB.2	21.51	40.12	11.96	2.82	0.61	0.37	1.06	12.1	0.76
Pearton (1986) - Albitites									
SC4	6.13	11	-	1.32	0.41	0.13	0.27		
SC5	6.36	15	-	1.17	0.34	0.14	-	12.1	0.76

Eu/Eu* = Chondrite normalized Eu value divided by the value obtained by drawing a line between Sm and Tb

Table 4.2.1. RARE EARTH ELEMENTS AS DETERMINED BY NEUTRON ACTIVATION ANALYSIS (ppm)

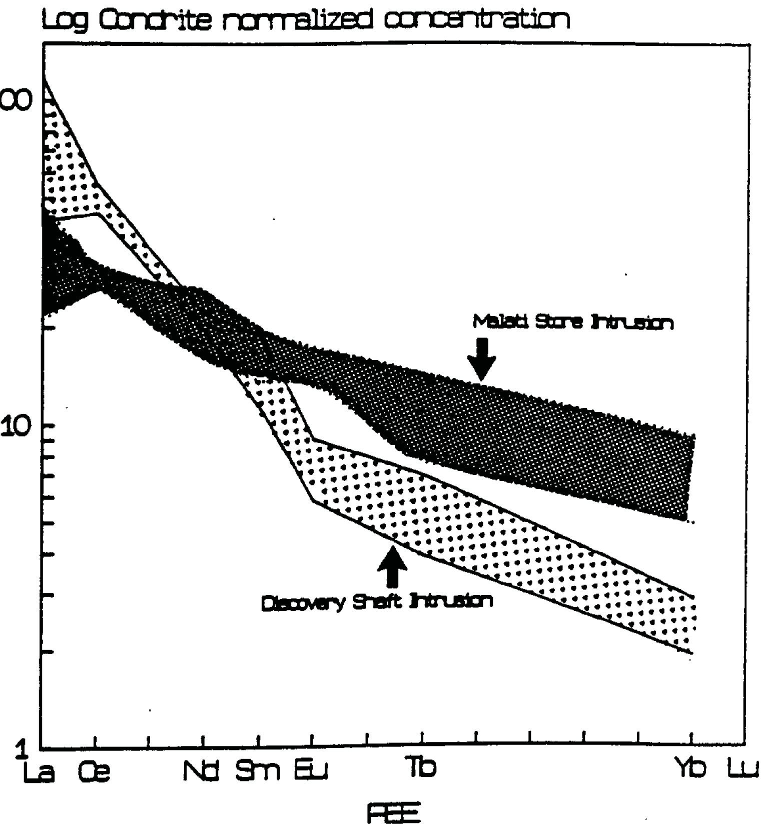

Figure 4.2.1. Chondrite normalized REE plot for the Malati Store and Discovery Shaft intrusions showing the envelope of distribution

The albitized Malati Store intrusion is enriched with HREE and slightly depleted in LREE, relative to the Discovery intrusion. Figure 4.2.2 shows that there is a systematic increase in the HREE content with a increasing degree of albitization (normative albite), which indicates that the HREE are selectively concentrated during alteration.

Unaltered granodiorites have a moderate to steep REE pattern, with a minor negative europium anomaly (Eu/Eu* =0.86). The average REE content of the moderately albitized Discovery Shaft intrusion is identical to that of the Willie pluton as indicated in Figure 4.2.3. This, along with other geochemical features, supports the idea that the albitized Discovery Shaft intrusion is genetically related to the Willie pluton or a geochemically similar granitoid. REE analyses in Vearncombe *et al.* (unpubl. data) show that the intrusive suite of granodiorites surrounding the Murchison schist belt have similar REE distributions to those of the intrusives examined in this study. The REE profiles of these granodiorite intrusions are considered to be representative of normal Archaean granodiorites (Taylor and McLennan, 1985).

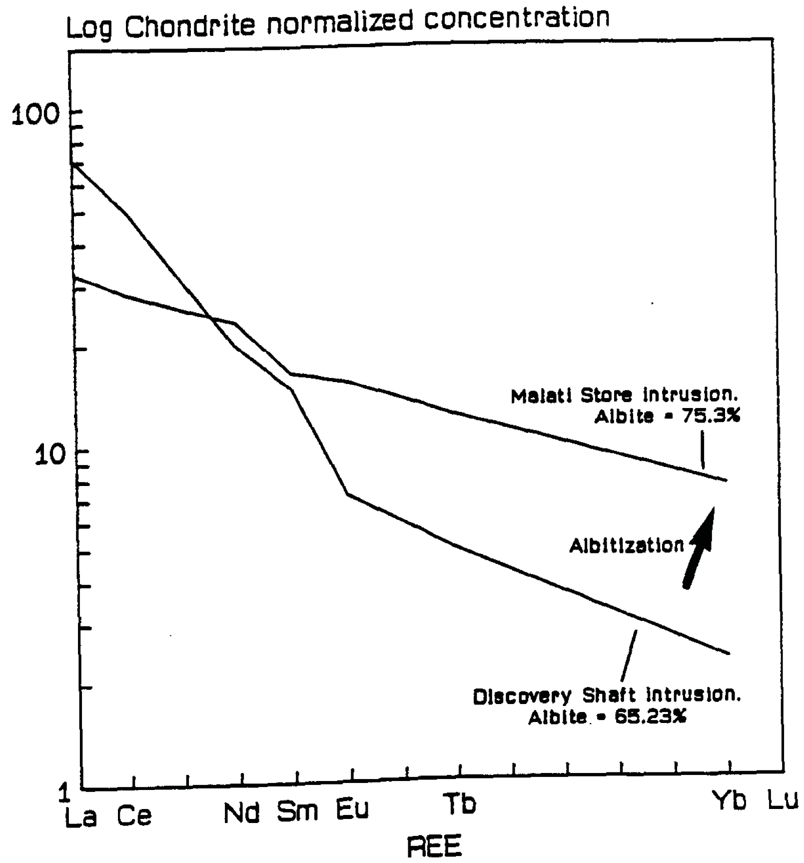

Figure 4.2.2. Chondrite normalized REE patterns for the albitized intrusions showing the increase in HREE with increased degrees of albitization

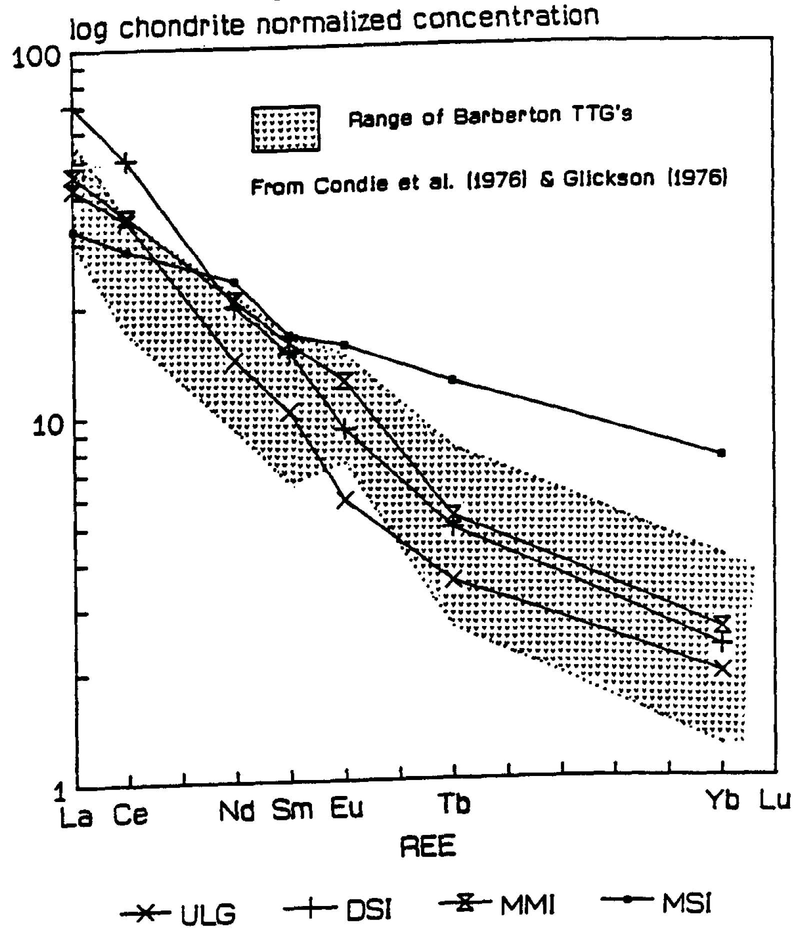

Figure 4.2.3. Average chondrite normalized REE patterns for the Willie Pluton (ULG), Discovery Shaft (DSI), Minerva Mine (MMI) and Malati Store (MSI) intrusions. REE range for the Barberton TTG's also included.

Figure 4.2.4. is a plot of the REE content of the Malati Store and Discovery Shaft intrusions normalized to the Willie pluton. There is a distinct increase in the HREE within the Malati Store intrusion as a result of the albitization.

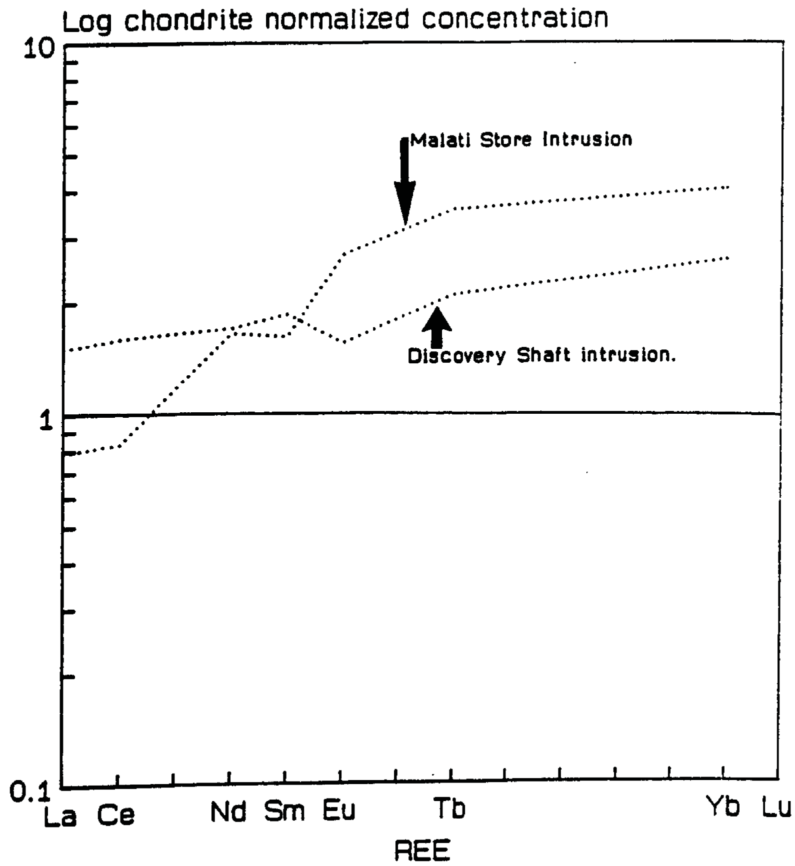

Figure 4.2.4. Log of the REE of the Malati Store (MMI) and Discovery Shaft (DSI) intrusions normalized to the Willie pluton. Note HREE enrichment.

The albite pegmatites from the Cobra pit at GEM have a LREE distribution similar to that of the Discovery Shaft intrusion and Willie pluton and also exhibit a slightly negative europium anomaly (Eu/Eu* =0.76). However the pegmatites are enriched in HREE relative to the Discovery Shaft and the Willie intrusion, and have a HREE distribution similar to that of the Malati Store intrusion. The LREE profile strongly suggests that there is a genetic relationship between the Willie Pluton and the albite-rich pegmatites which are responsible for emerald mineralization (Figure 4.2.5) as well as the albitized granodiorites. The albitite samples of Pearton (1980), from the borehole JLS.1 at Monarch North, are greatly depleted in REE, relative to the sample analyses of this study (Figure 4.2.6). It is unknown what these albite rich samples may represent. The "albitites" of Pearton (1980) do have similar smooth REE profiles.

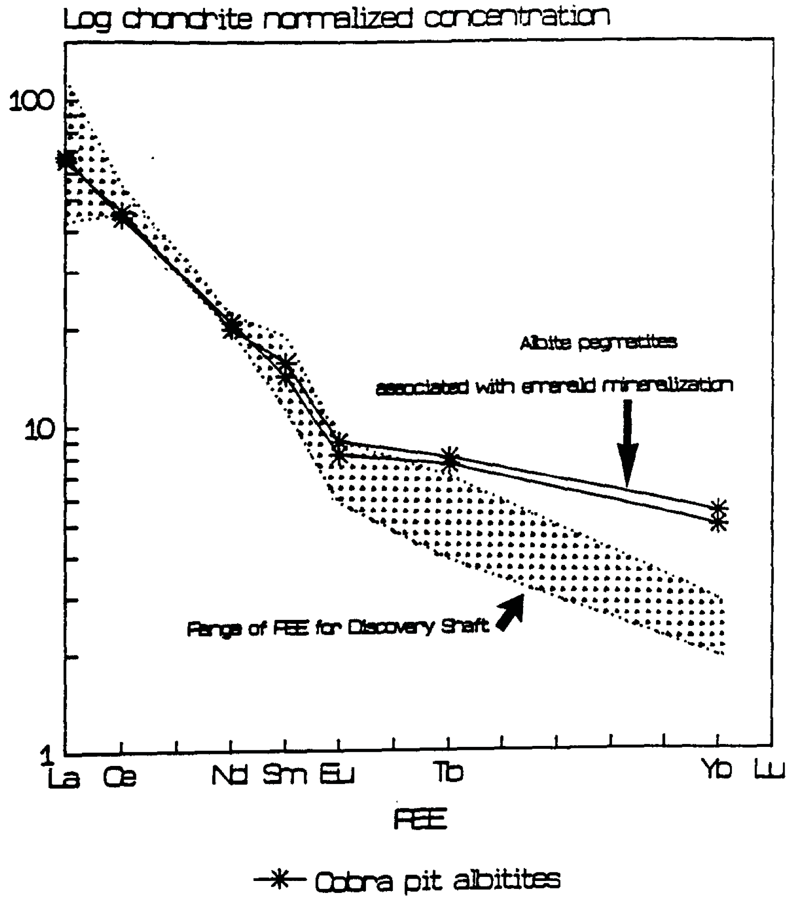

Figure 4.2.5. Chondrite normalized REE patterns for the albite pegmatites associated with emerald mineralization and the range of REE for the Discovery Shaft intrusion. Note the similarities in the LREE.

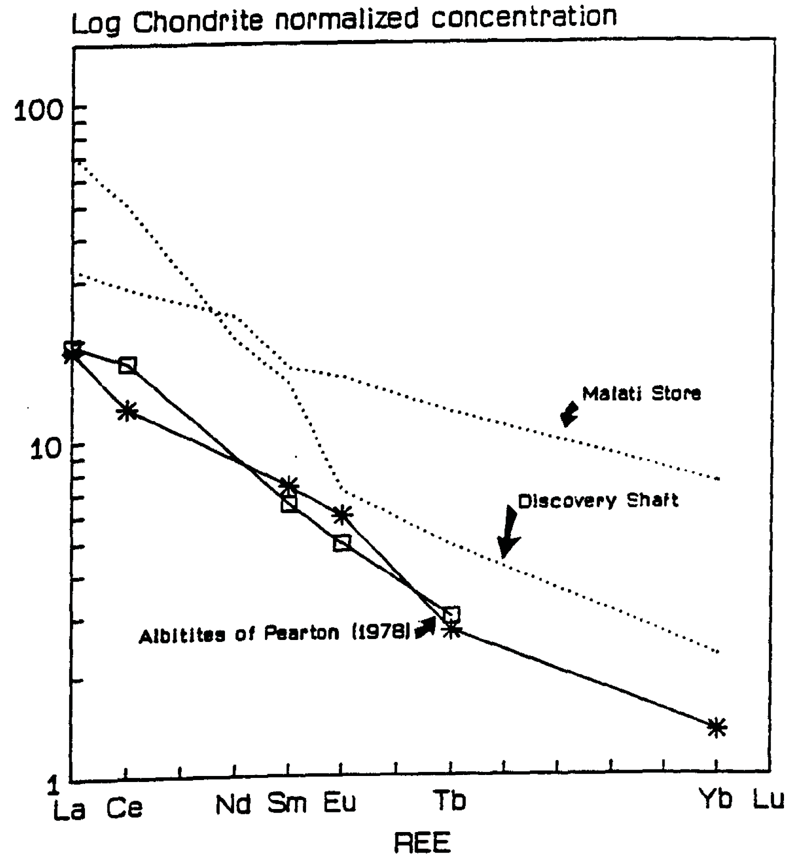

Figure 4.2.6. Chondrite normalized REE patterns of the albitites of Pearton (1980) compared to the average REE distribution of the Malati Store and Discovery Shaft intrusions

4.2.4. Discussion

The increase in HREE content with increased albitization indicates that these elements were preferentially concentrated into the fluid phase responsible for albitization. The rare earth content of hydrothermal solutions is controlled by the partitioning of REE between the solution and the mineral phases. However, quantitative solution / mineral or solution / melt partition coefficients are not available for the conditions prevalent in most hydrothermal systems. The REE content of hydrothermal fluids is generally very low, and thus in order to induces changes in the REE distribution of a rock, a large fluid to rock ratio is needed (generally in the excess of 10^2 to 10^3) (Taylor and Freyer, 1982). The REE pattern of the fluid involved in alteration is governed by the following;

1. The REE control of the host rock,
2. Sorption,
3. Complexation mechanisms, and
4. Relative stability of the secondary minerals.

REE enrichment is a common feature in peralkaline granites which have undergone sodium metasomatism (Jacobson *et al.* 1958; Mineyev, 1963; Aleksiyev, 1970). This is reconcilable with the activity of anionic species such as Cl^- F^- and CO_3^{-2} in these fluids, and with the formation of stable REE-bearing complexes with these ligands. The observed HREE enrichment probably, therefore, resulted from the transport of carbonate complexes in the alkali-enriched fluid responsible for metasomatism (Kerrich and Freyer, 1979). Fractionation of the REE in natural fluid systems typically affects the LREE relative to the HREE, or *vice versa*. This natural separation appears to be related to the formation and stability of the complexing ions (Moller *et al.*, 1979). Herrmann (1970) has suggested that complexing of REE with carbonates, fluorides or sulphate complexes could play a major role in the transport and deposition of the HREE. The increasing stability of these complexes with increasing atomic number of the REE results in the enrichment of the HREE in late stage deposits. During the waning stages of hydrothermal activity, REE complexes would destabilize, with subsequent precipitation of the complexed elements from the HREE enriched solution. The most probable complexing agent in the deposits in the present study is CO_3^{-2}, as suggested by the extensive carbonatization and the presence of CO_2 within fluid inclusions in hydrothermally deposited quartz. Experimental studies have shown that under near-neutral to mildly basic conditions the REE form soluble stable complexes (Kosterin, 1959; Graf, 1977; Alderton *et al.*, 1980), with the CO_3^{-2} complexes being the most important (Chatterjee and Strong, 1984; Taylor and Fryer, 1983). The stability of these